Prediction of cognitive decline in normal elderly subjects with 2-[^{18}F]fluoro-2-deoxy-D-glucose/positron-emission tomography (FDG/PET)

M. J. de Leon*†‡, A. Convit*†, O. T. Wolf*§, C. Y. Tarshish*, S. DeSanti*, H. Rusinek*, W. Tsui*, E. Kandil*, A. J. Scherer*, A. Roche*, A. Imossi*, E. Thorn*, M. Bobinski*, C. Caraos*, P. Lesbre*, D. Schlyer¶, J. Poirier‖, B. Reisberg*, and J. Fowler¶

*New York University School of Medicine, New York, NY 10016; †Nathan Kline Institute, Orangeburg, NY 10962; §University of Duesseldorf, Duesseldorf D-40225, Germany; ¶Brookhaven National Laboratory, Upton, NY 11973; and ‖McGill University, Montreal, QC, Canada H4H IR3

Edited by Marcus E. Raichle, Washington University School of Medicine, St. Louis, MO, and approved June 29, 2001 (received for review January 26, 2001)

Neuropathology studies show that patients with mild cognitive impairment (MCI) and Alzheimer's disease typically have lesions of the entorhinal cortex (EC), hippocampus (Hip), and temporal neocortex. Related observations with *in vivo* imaging have enabled the prediction of dementia from MCI. Although individuals with normal cognition may have focal EC lesions, this anatomy has not been studied as a predictor of cognitive decline and brain change. The objective of this MRI-guided 2-[^{18}F]fluoro-2-deoxy-D-glucose/positron-emission tomography (FDG/PET) study was to examine the hypothesis that among normal elderly subjects, EC METglu reductions predict decline and the involvement of the Hip and neocortex. In a 3-year longitudinal study of 48 healthy normal elderly, 12 individuals (mean age 72) demonstrated cognitive decline (11 to MCI and 1 to Alzheimer's disease). Nondeclining controls were matched on apolipoprotein E genotype, age, education, and gender. At baseline, metabolic reductions in the EC accurately predicted the conversion from normal to MCI. Among those who declined, the baseline EC predicted longitudinal memory and temporal neocortex metabolic reductions. At follow-up, those who declined showed memory impairment and hypometabolism in temporal lobe neocortex and Hip. Among those subjects who declined, apolipoprotein E E4 carriers showed marked longitudinal temporal neocortex reductions. In summary, these data suggest that an EC stage of brain involvement can be detected in normal elderly that predicts future cognitive and brain metabolism reductions. Progressive E4-related hypometabolism may underlie the known increased susceptibility for dementia. Further study is required to estimate individual risks and to determine the physiologic basis for METglu changes detected while cognition is normal.

With increasing age, there is an increased risk for memory impairment (1); however, the affected anatomy predicting future impairment has not been well characterized. Although many conditions result in memory loss, Alzheimer's disease (AD) may be the most common cause (2). Neuropathology studies of normal elderly and subjects with clinically recognizable mild cognitive impairments (MCI) show that both the entorhinal cortex (EC) and hippocampus (Hip), structures important for memory function, are particularly vulnerable to neurofibrillary tangle (NFT) pathology (3, 4) and neuronal loss (5). Braak and Braak (3) proposed a staging model for brain AD where the NFT distribution expands from an EC locus to involve the Hip and then the neocortex. Carriers of an apolipoprotein E (apoE) E4 allele show at younger ages increased neocortical beta amyloid deposits (6) and EC NFTs (7). These changes may contribute to their increased risk for AD.

In vivo, little is known of the regional anatomical changes marking the transitions between normal cognition and dementia. Although cross-sectional MRI and positron-emission tomography (PET) studies support an *in vivo* adaptation of the Braak staging model (8, 9), longitudinal imaging studies have not investigated the decline from normal. The decline from MCI to AD has been examined only. Reduced size or glucose metabolism (METglu) in the EC (10), Hip (11–16), temporal neocortex (17–20), and posterior cingulate gyrus (16) have been shown to predict the MCI conversion to AD. Moreover, both cross-sectional (21, 22) and longitudinal PET studies (23) show that nondemented E4 carriers have more hypometabolic regions than controls, but a relationship to longitudinally observed decline has not been reported.

By using MRI-guided PET sampling, the present longitudinal study of healthy normal elderly examined whether reduced baseline EC METglu predicted clinical decline and the longitudinal progression of hippocampal and neocortical METglu changes. The interaction of apoE genotype on brain and behavior was also studied.

Methods

Subject Screening and Diagnostic Examinations. In response to public announcements at the New York University–National Institutes of Health/National Institute on Aging AD Core Center, over a period of 6 years and after extensive baseline evaluations and screenings (see below), a 36-month follow-up MRI and PET study was completed. For MRI, 144 normal community-residing elderly were enrolled at the baseline of whom 105 completed the follow-up. At the baseline, 67/144 subjects were also enrolled in the PET study, of whom 48 completed the 36-month PET evaluation (see below). The clinical evaluations included medical (history, physical, and laboratory), neurologic, psychiatric, neuropsychologic tests, and MRI scans.

Exclusion Criteria. Conditions affecting brain structure or function (e.g., stroke, diabetes, head trauma, depression) or use of cognitively active medications led to exclusion at baseline or follow-up.

Inclusion Criteria. The subjects were between 60 and 80 years of age, had a minimum of 12 years education, received mini mental status examination (MMSE; ref. 24) scores $\geq$ 28, and, on a clinical interview based on the global deterioration scale (GDS;

This paper was submitted directly (Track II) to the PNAS office.

Abbreviations: MCI, mild cognitive impairment; GDS, global deterioration scale; METglu, glucose metabolism; EC, entorhinal cortex; DFL, dorsolateral frontal lobe; LTL, lateral temporal lobe; apoE, apolipoprotein E; FDG, 2-[^{18}F]fluoro-2-deoxy-D-glucose; SPM, statistical parametric mapping; NFT, neurofibrillary tangle; PET, positron-emission tomography; ROI, regions of interest; Hip, hippocampus.

‡To whom reprint requests should be addressed at: Center for Brain Health HN400, New York University School of Medicine, 560 First Avenue, New York, NY 10016. E-mail: mony.deleon@med.nyu.edu.

The publication costs of this article were defrayed in part by page charge payment. This article must therefore be hereby marked "*advertisement*" in accordance with 18 U.S.C. §1734 solely to indicate this fact.

www.pnas.org/cgi/doi/10.1073/pnas.191044198

Table 1. Demographic variables

	Outcome groups		ApoE groups	
	Non-Dec	Dec	E4−	E4+
No. of subjects	13	12	17	8
Age baseline, yrs	68 ± 5	72 ± 6	69 ± 6	72 ± 5
% Female	69	50	59	62
Education, yrs	16 ± 3	16 ± 2	16 ± 2	14 ± 3
FU, yrs	2.9 ± 0.4	3.0 ± 1.1	3.0 ± 1.0	2.8 ± 0.9
GDS baseline	1.9 ± 0.4	2.0 ± 0.0	2.0 ± 0.0	1.8 ± 0.5
GDS follow-up	1.9 ± 0.3	3.2 ± 0.6*	2.5 ± 0.5	2.6 ± 1.2
MMSE baseline	29.2 ± 1.1	29.3 ± 0.9	29.1 ± 1.0	29.4 ± 0.9
MMSE follow-up	29.5 ± 0.7	28.3 ± 2.1	29.1 ± 1.1	28.5 ± 2.4

Dec, decline; means ± SD; *, $P \leq 0.05$.

refs. 25 and 26) at baseline, received scores of 1 or 2. The evaluations for both time points were completed within a 3-month period after written informed consent was obtained at New York University and Brookhaven National Laboratory.

Outcome Groups. At baseline, none of the subjects demonstrated cognitive or functional deficits and all were diagnosed as normal. Normal subjects are assigned GDS scores of 2 or 1, depending on whether or not they report recent reductions in memory. At the 36-month follow-up, decline was defined by a GDS ≥ 3 on the basis of a clinical interview. An informant always corroborated the determination of decline. Individuals who receive a GDS of 3 show mild cognitive (typically memory) deficits that affect executive performance in complex social activities. These impairments are of insufficient magnitude to affect activities of daily living (ADL) or to meet National Institute of Neurological and Communicative Disorders and Stroke (NINCDS)–Alzheimer's Disease and Related Disorders Association (27) or the *Diagnostic and Statistical Manual of Mental Disorders IV* (28) criteria for AD or dementia. These patients are referred to as having MCI. A GDS ≥ 4 was assigned to individuals demonstrating ADL deficits and with clinically manifested decline in multiple cognitive domains. GDS ≥ 4 patients meet the criteria for dementia.

Of 48 subjects, 13 declined (all GDS = 2 at baseline and 4 heterozygote E4 carriers). From the 35 nondeclining subjects, 13 matched controls (11 GDS 2 and 2 GDS 1) were selected on (descending order of importance): E4 carrier or noncarrier, age, education, and gender (see Table 1). Among those who declined, 12 declined to MCI and 1 met criteria for probable AD (GDS = 5). One patient with MCI was excluded during the data analysis because a small thalamic lacunar infarct, not detected on the follow-up clinical MRI, was found on the follow-up research MRI.

Psychometric Evaluations

The psychometric battery was comprised of 10 tests administered in 2 sessions. These included the designs test [memory for abstract shapes (29)], the digit–symbol substitution test [an attention and psychomotor speed measure (30)], the confrontational object-naming test (31), the visual recognition memory test [a measure of visual memory span (31)], and the immediate and delayed recall of paragraphs (29), paired associates (29), and the shopping list [a selective reminding test (31)].

ApoE Genotyping. ApoE genotype was determined in the Poirier laboratory by using standard procedures (32).

Magnetic Resonance Imaging (MRI)

Acquisition Protocol. MRI scans were acquired by using a-1.5 T General Electric Signa imager. The clinical scan covered the entire brain with contiguous 3-mm axial T2-weighted and proton density-weighted images. The research MRI scan was a T1-weighted fast-gradient-echo with repetition time (TR) = 35 ms, echo time (TE) = 9 ms, and flip angle = 60° reconstructed into 124 contiguous slices. The research scan was acquired either as coronal 1.3-mm-thick images obtained perpendicular to the long axis of the Hip [field of view (FOV) = 18 cm, number of excitations (NEX) = 1, matrix = 256 × 128] or as sagittal 1.2-mm-thick images (FOV = 25 cm, NEX = 1, matrix = 256 × 128).

MRI images were aligned to a common spatial orientation, and the baseline and follow-up scans were coregistered (33). From mid-sagittal views of the coregistered data, 3.4-mm-thick coronal images were created perpendicular to a reference plane tangent to the base of the frontal and occipital lobes (34). To minimize MRI image degradation, the above were all completed in a single sinc interpolation step.

Regions of Interest (ROI). Blind to other data, 6 bilateral ROI were outlined by using gyral and sulcal landmarks. These included 4 temporal lobe regions (2 medial and 2 neocortical) and 2 frontal lobe regions. In addition, a large slab of tissue was used to normalize the regional METglu and reduce between-subject variability.

EC. We published anatomical guidelines for reliable and valid MRI sampling of the EC (34). On each of 5–7 coronal MRI slices, we outlined the EC gray matter. To improve the isotope recovery we enlarged this ROI to include an equal amount of adjacent white matter. This procedure resulted in ROI that were ≈1 cm in width by 2.5–3.5 cm in length. The anterior limit of the EC was 3.4 mm (1 slice) posterior to the frontal–temporal junction. The posterior limit was the anterior lateral geniculate body. The lateral boundary was the depth of the rhinal sulcus (anterior) or the collateral sulcus (posterior). The medial limit was the apex of the ambiens gyrus (anterior) or the uncus of the parahippocampal gyrus (posterior).

Hip. To maximize isotope recovery and reduce partial volume effects we restricted our published MRI protocol (35) to the 3–5 slices containing the pes Hip (9).

Lateral Temporal Lobe (LTL). This composite region, comprised of the middle and inferior temporal and fusiform gyri, spans from the anterior EC to the posterior crux of the fornix. It is bound superiorly by the superior temporal sulcus and inferiorly by the rhinal or collateral sulcus.

Superior temporal gyrus. The region shares the LTL span and is bound by the sylvan fissure and the superior temporal sulcus.

The dorsolateral frontal lobe (DFL). The middle frontal gyrus, bound by the middle and inferior frontal sulci, was sampled on three consecutive slices. The anterior limit was defined by the genu of the corpus callosum.

The orbital frontal lobe (OFL). The OFL was sampled by using the same anterior and posterior limits as the DFL. The sample included the gyrus rectus and the medial orbital gyrus.

Reference tissue slab. The slab encompassed the entire anterior–posterior (A–P) span of the temporal lobe drawings. It spanned both hemispheres from left to right dural margins. The 3-cm-tall slab was positioned inferior to the third ventricle. It included the basal ganglia and portions of the superior temporal gyrus and excluded Hip, EC, and LTL regions that were part of our hypotheses.

PET Studies

Acquisition Protocol. PET scans, using 2-[^{18}F]fluoro-2-deoxy-D-glucose (FDG), were obtained with a Siemens (Iselin, NJ) CTI-931 scanner. The scanner generates 15 axial-contiguous 6.7-mm slices covering 101 mm, with 6.2-6.7-mm full-width at half maximum (FWHM) resolution. Each subject's head was secured with a custom-molded head holder. Attenuation correction was made by using a ^{68}Ga/^{68}Ge transmission scan.

One hour before the PET scan, a radial artery catheter and a

PSYCHOLOGY

Table 2. Cross-sectional and METglu data: slab normalized regional means (mean and SD values × 100)

	Outcome group						ApoE group					
	Baseline			Follow-up			Baseline			Follow-up		
Regions	Non-Dec	Dec	*P*	Non-Dec	Dec	*P*	E4−	E4+	*P*	E4−	E4+	*P*
EC	91 ± 7	75 ± 7	+	86 ± 5	71 ± 7	+	84 ± 10	81 ± 12		80 ± 8	76 ± 12	
Hip	90 ± 6	87 ± 5		86 ± 5	80 ± 11	*	88 ± 5	90 ± 7		84 ± 8	82 ± 10	
STG	105 ± 3	103 ± 4		103 ± 5	100 ± 9		105 ± 3	102 ± 4	*	103 ± 4	99 ± 11	
LTL	97 ± 7	91 ± 8		93 ± 4	86 ± 13	+	97 ± 6	89 ± 9	*	93 ± 4	83 ± 16	+
OFL	101 ± 15	102 ± 8		105 ± 6	100 ± 12		101 ± 14	102 ± 8		104 ± 10	100 ± 9	
DFL	117 ± 9	109 ± 12		120 ± 7	113 ± 9		113 ± 13	114 ± 7		118 ± 8	113 ± 10	

STG, superior temporal gyrus; OFL, orbital frontal lobe; Dec, decline. *, $P \leq 0.05$; +, $P \leq 0.01$.

contralateral antecubital venous line were positioned. Subjects received 5–6 mCi of FDG intravenously. During the scan, subjects lay supine in the dimly lit scanner room with their eyes open and ears unoccluded. Scanning commenced 35 min after isotope injection and lasted for 20 min. To reduce isotope recovery errors associated with reformatting the PET data from the axial to the coronal plane, we obtained and interleaved two 15-slice data acquisitions that were translated by a half-slice thickness (≈3.4 mm; ref. 36). Quantitative METglu images were calculated from emission data and arterial blood samples (37).

PET/MRI Image Registration. Each PET scan was coregistered with the corresponding MRI by using a three-dimensional method based on minimizing the variance of the signal ratios (33). Our implementation calls for a preliminary spatial alignment, using intrinsic anatomical landmarks. We estimated an average registration error of <2 mm.

The Regional METglu. After registration, the PET images were sampled by using the MRI ROI. Metabolic means (μmol/100 g/min) were computed for each ROI across all slices sampled. These regional values were averaged across hemispheres and normalized by creating a ratio with the reference slab values as the denominator. We also simulated recovery coefficients for our ROI with variable background gray and white matter contrasts (36). The results show that the regional isotope recovery is robust and varies in a narrow (<5% absolute error) range. Moreover, using the method of Rousset (38), we observed <9% metabolic cross talk between the Hip and EC. Therefore, we consider these regional samples to be independent.

Atrophy Correction of Metabolic Activity. The coregistered PET scans were corrected for the partial volume of cerebrospinal fluid (CSF) by using a method of Meltzer (9). The application of this correction increased regional metabolism by 10–21% in those who declined and 5–15% in those who did not decline, with the greatest adjustment seen in EC and DFL, respectively. E4 carriers showed 11–17% adjustment as compared with 6–14% in the noncarriers. The greatest adjustments were for the EC.

Statistical Parametric Mapping (SPM). To extend the analysis to the whole brain, we also computed voxel-based effects by using SPM99 (Wellcome Department of Cognitive Neurology, London). PET images were spatially registered, normalized to the metabolism of the slab, smoothed with a 14-mm Gaussian kernel, studied with a cluster size ≥10, and adjusted for multiple comparisons ($P < 0.01$).

Statistical Analyses. The basic statistical model for the cross-sectional analyses was a two-factor ANOVA. The factors were outcome group (declining vs. nondeclining subjects) and apoE group (E4 carriers vs. noncarriers). For tests of the longitudinal hypotheses, the two factors were examined in a repeated-measures model. Hierarchical linear and logistic regression models were used to predict outcome. Also separately examined were the effects of removal of the case with AD (E4 carrier) from the analyses and atrophy correction. The SPM results were examined with pixel-wise *t* tests.

Results

Demographic Data. At the 36-month follow-up, cognitive decline was seen in 29% of the 105 MRI subjects, which was comparable to the 27% observed in the 48 PET subjects. Confirming the PET study matching procedure, at baseline when all subjects were normal, no demographic differences were found between outcome groups (see Table 1). Time to follow-up was equivalent.

Brain METglu Findings

Baseline Effects. The EC METglu was reduced 18% in those who declined relative to those who did not decline ($F[1,21] = 29.1$, $P < 0.001$; see Table 2). Both the LTL and the superior temporal gyrus were reduced in E4 carriers relative to noncarriers (8%, $F[1,21] = 6.9$, $P = 0.05$; and 3%, $F[1,21] = 4.6$, $P = 0.05$, respectively). After removal of the case that later declined to AD, only the EC outcome group effect remained significant (17%, $P < 0.001$). With atrophy correction the EC outcome group effect (11%, $P < 0.01$) and the LTL apoE effect (8%, $P < 0.01$) remained significant, and the DFL METglu became significantly reduced in those who declined (10%, $F[1,21] = 4.7$, $P < 0.05$). SPM did not show any area with significant main effects. None of the analyses showed an interaction between outcome and apoE groups.

Univariate Baseline Predictions. The EC correctly classified decline outcome with 84% accuracy: 83% sensitivity (those who declined) and 85% specificity (those who did not decline) [X^2 (1) = 20.8, $P < 0.001$; odds ratio = 1.42; confidence interval (CI) = 1.08–1.88]. Removing the one case with AD or correcting for atrophy had little effect on the EC classification (83 and 80%, respectively). Although the mean atrophy corrected DFL, METglu was significantly reduced in those who declined. This measure did not significantly contribute to the risk for decline (lower CI limit ≤ 1.00).

Follow-Up Effects. The declining group showed significantly lower METglu in EC (17%, $F[1,21] = 35.5$, $P < 0.001$), Hip (7%, $F[1,21] = 4.5$, $P < 0.05$), and LTL (8%, $F[1,21] = 8.0$, $P = 0.01$). After removal of the case with AD, significant outcome effects remained for the EC (16%, $P < 0.001$) and LTL (5%, $P < 0.05$). No apoE by outcome group interactions were found with or without the case with AD. With atrophy correction, the declining group had lower ($P < 0.05$) METglu in the EC (9%), DFL (10%), and LTL (6%). Also after correction, the LTL showed an interaction between outcome and apoE groups ($F[1,21] = 5.4$, $P < 0.05$), where those who declined that were E4 carriers

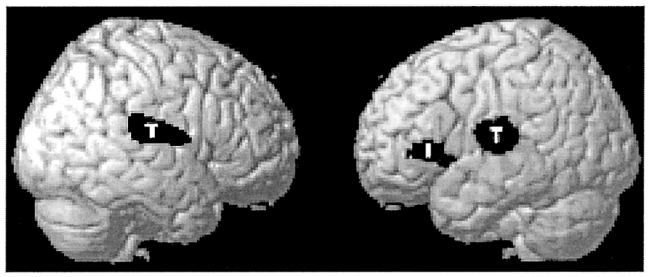

Fig. 1. PET voxels that demonstrate (at follow-up) reductions in METglu. Significant clusters are shown in black over a rendered brain surface. T, lateral temporo-parietal area; I, inferior frontal gyrus.

showed lower METglu than those who declined who were not carriers.

The SPM analyses for outcome group showed clusters of metabolism reduction for those who declined bilaterally in the temporo-parietal cortex and the left inferior frontal gyrus. Maximal metabolic reductions for each of these clusters, in Talairach space (x, y, and z), were -38, -20, and 6; 44, -12, and 14; and -40, 22, and 4, respectively (see Fig. 1). There were no apoE group effects or interactions.

Longitudinal Effects. No regional longitudinal main effects were found. However, the LTL showed a significant longitudinal outcome by apoE group interaction [$F(1,21) = 7.2, P = 0.01$]. E4 carriers that declined showed reductions of 13% over time relative to 3% in those who declined not carrying an E4 allele (see Fig. 2). The LTL interaction was also found after removal of the case with AD ($P = 0.05$) and after atrophy correction ($P = 0.01$). No significant longitudinal main effects or interactions were found with SPM.

The Prediction of Longitudinal Brain Change. The EC at baseline (the predictor of clinical decline) was examined as a predictor of longitudinal change in the METglu of other brain regions. These analyses were done for the total sample and separately for each outcome and apoE group. Only among those who declined did a smaller baseline EC predict greater longitudinal reduction in the LTL [$F(1,9) = 5.0$, $P < 0.05$] and the orbital frontal lobe [$F(1,9) = 6.0$, $P < 0.05$]. After removing the case with AD or atrophy correction, the relationship between the baseline EC and the LTL remained significant.

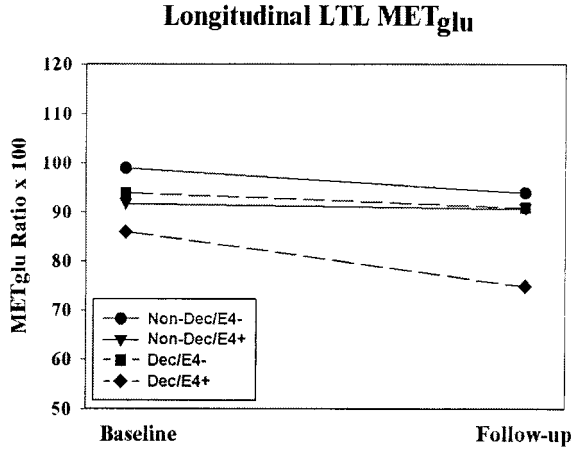

Fig. 2. Average normalized LTL METglu for baseline and follow-up periods. The results show a significant longitudinal interaction between outcome (decline vs. nondecline) and apoE groups (E4 carriers vs. noncarriers). Dec, decline; E4 +/−, carriers/noncarriers of an apoE E4 allele.

Neuropsychological Findings

Baseline Effects. Only the designs test was different between outcome groups (see Table 3). No apoE effects or interactions between outcome and apoE groups were found for any of the measures. These results were unchanged after removal of the case that later became AD.

Baseline Prediction Effects. The designs measure weakly predicted decline [68%, $P < 0.05$; odds ratio = 1.62, confidence interval (CI) = 1.00–2.60]. The overall classification accuracy was identical after removal of the case with AD. In a regression model, adding the uncorrected baseline EC to the designs test increased the number of cases correctly classified but did not significantly increment the risk for decline (lower CI limit < 1.00).

Follow-Up Effects. At follow-up, the declining group showed significant ($P < 0.05$) reductions in 8/10 neuropsychological measures and a trend toward reduced MMSE performance ($P < 0.1$). Two delayed-recall measures showed E4-related reductions but there were no outcome by apoE group interactions. After removal of the case with AD, the remaining MCI group performed more poorly on 6/10 measures; the immediate- and delayed-paragraph recall scores were no longer different (Ps > 0.05).

Longitudinal Effects. Significant outcome group effects were observed for the immediate [$F(1,20) = 5.8$, $P < 0.05$] and delayed retrieval of the shopping-list task [$F(1,20) = 5.3$, $P < 0.05$]. Within the declining group, the baseline EC predicted the longitudinal change in the immediate recall [$F(1,8) = 13.7$, $P < 0.01$] and the DFL predicted the change in the designs test [$F(1,9) = 14.0$, $P < 0.01$]. After removal of the case with AD, the delayed retrieval of the shopping-list test continued to show a longitudinal outcome effect [$F(1,19) = 4.9$, $P < 0.05$], and the DFL remained a predictor of longitudinal designs performance [$F(1,8) = 5.7$, $P < 0.05$]. No apoE group effects or interactions were observed in any of the analyses.

Discussion

This longitudinal FDG/PET study is the first imaging study, to our knowledge, to predict future cognitive decline and MCI among normal elderly. Decreased EC METglu at baseline was the most accurate regional predictor of clinical change.

The neuropathology of AD is known to involve the EC in normal subjects (5) and also the Hip in MCI patients (39), findings supporting the Braak and Braak (3) staging of NFT accumulations. However, very little information is available *in vivo*. Few imaging studies have examined multiple vulnerable brain regions, and even fewer studies used longitudinal designs with patients who clinically decline (necessary because imaging outcome measures lack neuropathologic specificity).

Among structural imaging studies examining the conversion of MCI to AD, there are one longitudinal (40) and several prediction studies (one scan predicting clinical outcome). They report useful hippocampal (11–14), EC (10), and combined medial temporal and temporal neocortex (17) predictors for the conversion. Evidence suggesting that hippocampal volume reductions in MCI may characterize a clinical-anatomical stage that precedes dementia and neocortical atrophy comes only from cross-sectional data (8). Consequently, from the structural imaging literature, it remains largely unexplored whether neocortical changes in addition to medial temporal changes are necessary for decline to AD.

Metabolic prediction imaging studies examining the conversion of MCI to AD, with one exception, have not examined the Hip. The recent SPECT study by Johnson *et al.* (16) demonstrated that reduced perfusion of the Hip and posterior cingulate

Table 3. Cross-sectional cognitive test scores by outcome groups (mean and SD values)

	Outcome group						ApoE group					
	Baseline			Follow-up			Baseline			Follow-up		
Tests	Non-Dec	Dec	*P*	Non-Dec	Dec	*P*	E4−	E4+	*P*	E4−	E4+	*P*
Para-I	7.4 ± 1.8	6.2 ± 2.5		7.4 ± 2.3	5.4 ± 2.4	*	6.9 ± 2.4	6.7 ± 2.0		6.9 ± 2.2	5.4 ± 2.9	
Para-D	9.5 ± 2.6	7.4 ± 3.5		8.4 ± 2.1	6.0 ± 4.0	*	8.7 ± 3.6	8.0 ± 2.5		8.1 ± 3.1	5.6 ± 3.4	+
Assc-I	5.5 ± 2.9	4.1 ± 3.6		6.7 ± 3.0	4.3 ± 3.5		5.1 ± 3.3	4.4 ± 3.3		6.2 ± 3.3	4.2 ± 3.4	
Assc-D	6.5 ± 3.4	4.7 ± 3.5		7.8 ± 2.8	4.1 ± 3.4	+	6.2 ± 3.2	4.2 ± 3.8		6.8 ± 3.2	4.4 ± 3.9	
Designs	7.5 ± 1.6	5.6 ± 2.5	+	7.8 ± 2.3	4.2 ± 3.0	+	6.6 ± 2.2	6.6 ± 2.7		6.1 ± 3.0	6.2 ± 3.8	
DSST	58.2 ± 9.3	48.9 ± 15.0		59.2 ± 10.4	48.8 ± 9.9	*	53.8 ± 14.2	53.5 ± 10.9		54.7 ± 10.5	53.0 ± 13.4	
Object	55.6 ± 5.1	47.0 ± 18.0		57.7 ± 3.6	46.9 ± 16.6	*	50.9 ± 15.7	53.6 ± 4.5		54.9 ± 7.4	43.7 ± 21.9	
Shop-I	7.1 ± 1.3	6.3 ± 1.6		7.8 ± 1.7	5.6 ± 2.1	+	6.9 ± 1.6	6.4 ± 1.2		7.2 ± 2.0	5.6 ± 2.4	
Shop-D	8.7 ± 1.3	7.7 ± 2.1		9.3 ± 1.0	6.8 ± 3.0	+	8.5 ± 1.7	7.8 ± 1.8		8.7 ± 1.7	6.8 ± 3.4	*
Recog	16.8 ± 10.0	14.6 ± 9.0		15.7 ± 9.7	13.8 ± 8.3		16.1 ± 8.9	15.2 ± 11.0		16.1 ± 8.9	12.4 ± 9.0	

Dec, decline; I, immediate recall; D, delayed recall; Para, paragraph; Assc, paired associate; DSST, digit symbol substitution test; Object, object naming; Shop, shopping list; Recog, visual recognition; E4+, carrier; E4−, noncarrier; *, $P \leq 0.05$; +, $P \leq 0.01$.

gyrus predicted AD. Others have observed that temporoparietal METglu deficits predict AD (18–20). However, as with MRI, evidence that focal hippocampal metabolic alterations are characteristic of MCI comes only from cross-sectional data (9). Overall, the metabolic imaging literature suggests that a more widespread pattern of involvement predicts the decline from MCI to AD.

The results of the present longitudinal metabolic imaging study support a recognizable EC stage among normal elderly in advance of clinical decline. We did not observe the development or progression of EC changes in our cohort, therefore, our results indicate that the EC reductions occurred before our study began. This result suggests that although EC pathology may be a specific predictor, it alone does not cause the decline from normal. At follow-up, we saw development of the hippocampal and neocortical metabolic reductions in the patients who declined. We also observed that among those who declined the baseline EC predicted both longitudinal reductions in LTL METglu and memory performance. However, because the between-group brain changes detected at follow-up failed to significantly change between baseline and follow-up, it is premature to state that LTL changes caused the decline. Although our findings are consistent with experimental baboon EC lesion data reported by Meguro *et al.* (41), we do not know whether the metabolic reductions we detected at follow-up were caused by progressive AD lesions or by an impoverished neural network after EC damage. Overall, our results suggest that in the conversion of normal to MCI, EC changes occur in advance of decline and other regional changes.

Our data do not support a Hip-specific stage after the EC stage. At the follow-up, the impaired individuals showed a strong effect in temporal neocortical regions. This effect was more robust than the bilateral hippocampal effect that disappeared after removing the one case that declined to AD. Because of this unexpected finding, we examined the unilateral differences in this region and found a right hippocampal reduction in the MCI group at follow-up [9%, $F(1,20) = 8.9$, $P < 0.01$]. This unilateral effect too was not significant as a longitudinal effect. Overall, these data suggest that 3 years were not a long enough follow-up interval to observe the hypothesized longitudinal hippocampal involvement.

Etiologic heterogeneity is suspected in MCI, and it is not known how this may have contributed to our findings. Not all subjects with MCI deteriorate to clinical AD. Estimates based on 4 years of observation suggest that 50–70% will decline (42). Relatedly, in the absence of a specific diagnostic test, it is also unknown what proportion of patients with MCI have AD neuropathological changes [estimates range as high as >80% (39)]. Continued follow-up of our cohort may reveal the utility of the EC, Hip, and other regions to predict decline to clinically recognizable AD.

The mechanism by which AD-related brain changes effect METglu is not known. Patients with AD show numerous lesions that may explain the hypometabolism—synaptic and neuronal losses and amyloid and NFT depositions (see ref. 43 for summary). Furthermore, the mechanism by which the apoE genotype influences brain METglu is unknown. *In vitro*, β-amyloid has been shown to reduce glucose transport (43), and one can speculate that the excess temporal neocortex metabolic reduction found in E4 carriers is related to increased β-amyloid deposition (6). This conjecture is supported further by the increased predilection in early AD for β-amyloid to accumulate in the neocortex rather than the hippocampal formation (2, 6) and by reductions in METglu observed in transgenic mouse models overproducing amyloid (44). NFT depositions, on the other hand, damage neurons (45), favor the hippocampal formation over the neocortex in preclinical AD stages (3, 4), and may also be accelerated in E4 carriers (7). Consequently, we expected that the metabolism of the EC (the region that best predicts clinical decline) and the LTL (the most affected neocortical region at the follow-up) would both demonstrate apoE group by outcome group interactions. The results show that only the LTL showed the interaction, which on closer examination was driven by declining E4 carriers (all heterozygous). Although we cannot at this time offer an E4-related mechanism that effects metabolism, our data add to previous reports by demonstrating an association between genotype, METglu, and cognitive decline. It has been suggested that this association may account for the earlier onset of symptoms in E4 carriers (21–23).

As expected, correction of the regional metabolism samples for the partial volume of cerebrospinal fluid generally increased the values. However, these corrections did not affect our main conclusions. The DFL, an exception, showed after correction a significant outcome group effect. Although hierarchical regression analyses showed the DFL reduction to be inferior to the EC in the prediction of cognitive decline, DFL changes may explain some of the memory and attention changes seen in aging. Neuropsychological studies (see ref. 46 for review) and neuroimaging studies (47) have often suggested that DFL changes underlie age-associated deficits in working memory, psychomotor speed, and attention. The pathological basis for the DFL metabolic reductions we observed is unknown, as histology studies have not critically examined the DFL in normal aging and early sporadic AD. Continued follow-up examination of our subjects is necessary to determine whether the DFL and EC,

regions that predict cognitive decline, will independently predict AD or other outcomes.

The uncorrected data were examined by using both ROI and SPM methods and the results demonstrate partial agreement between them. At baseline, neither approach identifies neocortical outcome group effects or interactions, but the ROI method showed small apoE group effects for the temporal neocortex. At follow-up, both methods show comparable neocortical outcome and apoE groups effects, but SPM uniquely identified an outcome group difference in the left inferior frontal gyrus, a region not studied with ROI. Importantly, the ROI method identified EC outcome group effects at baseline and follow-up that were not found with SPM. Our findings suggest that the SPM spatial normalization algorithm may not be capable of aligning the EC, a region with large anatomical variability, across individuals in a consistent manner.

In conclusion, baseline measures of EC METglu in normal elderly predicted the conversion from normal to MCI. Among those who declined, the baseline EC predicted longitudinal memory and neocortical metabolic reductions. Consistent with the neuropathological model proposed by Braak and Braak (3), these data suggest an EC stage of brain involvement that can be detected in normal elderly. However, at follow-up, we did not observe a specific hippocampal stage associated with MCI; instead, we found neocortical temporal lobe hypometabolism and limited hippocampal involvement. Longitudinally, declining E4 carriers showed marked neocortical temporal lobe reductions. Therefore, progressive E4-related hypometabolism may underlie the known E4 carrier's increased susceptibility for dementia. Continued study is required to determine the clinical utility and the pathologic and physiologic bases of METglu reductions in cognitively normal individuals. We caution that our observations were made with small numbers of subjects under controlled conditions; clinical application is not yet justified.

We dedicate this paper to the memory and scientific contributions of our dear friend and colleague, Professor Eva Braak of Frankfurt, Germany. We thank Donald Warner; Robert Carciello for PET and cyclotron operations; Noelwah Netusil and Pauline Carter for subject care during the PET procedure; and Richard Ferrieri, David Alexoff, Colleen Shea, and Robert MacGregor for 2-[^{18}F]fluoro-2-deoxy-D-glucose synthesis. We thank Drs. Carl Campbell, Steven Ferris, and Blas Frangione for their constructive comments. This work was supported in part by National Institutes of Health-National Institute on Aging Grants AG13616, AG12101, AG03051, and AG08051; Deutsche Forschungsgesellschaft Grant WO 733/1-1 (to O.T.W.); the Canadian Institute for Health Research; and by the Alzheimer Society of Canada (to J.P.).

1. Larrabee, G. J. & Crook, T. H. (1994) *Int. Psychogeriatr.* **6,** 95–104.
2. Berg, L., McKeel, D. W., Miller, P. J., Storandt, M., Rubin, E. H., Morris, J. C., Baty, J., Coats, M., Norton, J., Goate, A. M., *et al.* (1998) *Arch. Neurol. (Chicago)* **55,** 326–335.
3. Braak, H. & Braak, E. (1991) *Acta Neuropathol.* **82,** 239–259.
4. Arriagada, P. V., Marzloff, K. & Hyman, B. T. (1992) *Neurology* **42,** 1681–1688.
5. Gomez-Isla, T., Price, J. L., McKeel, D. W., Jr., Morris, J. C., Growdon, J. H. & Hyman, B. T. (1996) *J. Neurosci.* **16,** 4491–4500.
6. Schmechel, D. E., Saunders, A. M., Strittmatter, W. J., Crain, B. J., Hulette, C. M., Joo, S. H., Pericak-Vance, M. A., Goldgaber, D. & Roses, A. D. (1993) *Proc. Natl. Acad. Sci. USA* **90,** 9649–9653.
7. Ghebremedhin, E., Schultz, C., Braak, E. & Braak, H. (1998) *Exp. Neurol.* **153,** 152–155.
8. Convit, A., de Leon, M. J., Tarshish, C., De Santi, S., Tsui, W., Rusinek, H. & George, A. E. (1997) *Neurobiol. Aging* **18,** 131–138.
9. De Santi, S., de Leon, M. J., Rusinek, H., Convit, A., Tarshish, C. Y., Boppana, M., Tsui, W. H., Daisley, K., Wang, G. J. & Schlyer, D. (2001) *Neurobiol. Aging* **22,** 529–539.
10. Killiany, R. J., Gomez-Isla, T., Moss, M., Kikinis, R., Sandor, T., Jolesz, F., Tanzi, R., Jones, K., Hyman, B. & Albert, M. S. (2000) *Ann. Neurol.* **47,** 430–439.
11. de Leon, M. J., George, A. E., Stylopoulos, L. A., Smith, G. & Miller, D. C. (1989) *Lancet* **2,** 672–673.
12. de Leon, M. J., Golomb, J., George, A. E., Convit, A., Tarshish, C. Y., McRae, T., De Santi, S., Smith, G., Ferris, S. H., Noz, M., *et al.* (1993) *Am. J. Neuroradiol.* **14,** 897–906.
13. Jack, C. R., Jr., Petersen, R. C., Xu, Y. C., O'Brien, P. C., Smith, G. E., Ivnik, R. J., Boeve, B. F., Waring, S. C., Tangalos, E. G. & Kokmen, E. (1999) *Neurology* **52,** 1397–1403.
14. Visser, P. J., Scheltens, P., Verby, F. R. J., Schmand, B., Launer, L. J., Jolles, J. & Jonker, C. (1999) *J. Neurol.* **246,** 477–485.
15. Ouchi, Y., Nobezawa, S., Okada, H., Yoshikawa, E., Futatsubashi, M. & Kaneko, M. (1998) *Neurology* **51,** 136–142.
16. Johnson, K. A., Jones, K., Holman, B. L., Becker, B. S., Spiers, P. A., Satlin, A. & Albert, M. S. (1998) *Neurology* **50,** 1563–1571.
17. Convit, A., de Asis, J., de Leon, M. J., Tarshish, C., De Santi, S. & Rusinek, H. (2000) *Neurobiol. Aging* **21,** 19–26.
18. Pietrini, P., Azari, N. P., Grady, C. L., Salerno, J. A., Gonzalez-Aviles, A., Heston, L. L., Pettigrew, K. D., Horwitz, B., Haxby, J. V. & Schapiro, M. B. (1993) *Dementia* **4,** 94–101.
19. Berent, S., Giordani, B., Foster, N., Minoshima, S., Lajiness-O'Neill, R., Koeppe, R. & Kuhl, D. E. (1999) *J. Psychiatr. Res.* **33,** 7–16.
20. Arnaiz, E., Jelic, V., Almkvist, O., Wahlund, L.-O., Winblad, B., Valind, S. & Nordberg, A. (2001) *NeuroReport* **12,** 851–855.
21. Small, G. W., Mazziotta, J. C., Collins, M. T., Baxter, L. R., Phelps, M. E., Mandelkern, M. A., Kaplan, A., LaRue, A., Adamson, C. F., Chang, L., *et al.* (1995) *J. Am. Med. Assoc.* **273,** 942–947.
22. Reiman, E. M., Caselli, R. J., Yun, L. S., Chen, K., Bandy, D., Minoshima, S., Thibodeau, S. N. & Osborne, D. (1996) *N. Engl. J. Med.* **334,** 752–758.
23. Small, G. W., Ercoli, L. M., Silverman, D. H. S., Huang, S. C., Komo, S., Bookheimer, S., Lavretsky, H., Miller, K., Siddarth, P., Rasgon, N. L., *et al.* (2000) *Proc. Natl. Acad. Sci. USA* **97,** 6037–6042. (First Published May 16, 2000; 10.1073/pnas.090106797)
24. Folstein, M. F., Folstein, S. E. & McHugh, P. R. (1975) *J. Psychiatr. Res.* **12,** 189–198.
25. Reisberg, B., Ferris, S. H., de Leon, M. J. & Crook, T. (1982) *Am. J. Psychiatry* **139,** 1136–1139.
26. Reisberg, B., Sclan, S. G., Franssen, E. H., de Leon, M. J., Kluger, A., Torossian, C. L., Shulman, E., Steinberg, G., Monteiro, I., McRae, T., *et al.* (1993) *Neurosci. Res. Commun.* **13,** Suppl. 1, 551–554.
27. McKhann, G., Drachman, D., Folstein, M., Katzman, R., Price, D. & Stadlan, E. M. (1984) *Neurology* **34,** 939–944.
28. American Psychiatric Association (1994) *Diagnostic and Statistical Manual of Mental Disorders* (Am. Psychiatr. Assoc., Washington, DC), 4th Ed.
29. Gilbert, J. G., Levee, R. F. & Catalano, F. L. (1968) *Percept. Mot. Skills* **27,** 277–278.
30. Wechsler, D. (1981) *Wechsler Adult Intelligence Scale–Revised* (Harcourt, Brace & Jovanovich, New York).
31. Flicker, C., Ferris, S. H. & Reisberg, B. (1993) *J. Geriatr. Psychiatry Neurol.* **6,** 84–96.
32. Main, R. F., Jones, P. J. H., McGillivery, R. T. A. & Banfield, D. K. (2000) *J. Lipid Res.* **1991,** 183–187.
33. Woods, R. P., Mazziotta, J. C. & Cherry, S. R. (1993) *J. Comput. Assist. Tomogr.* **17,** 536–546.
34. Bobinski, M., de Leon, M. J., Convit, A., De Santi, S., Wegiel, J., Tarshish, C. Y., Saint-Louis, L. A. & Wisniewski, H. H. (1999) *Lancet* **353,** 38–40.
35. Bobinski, M., de Leon, M. J., Wegiel, J., De Santi, S., Convit, A. & Wisniewski, H. M. (2000) *Neuroscience* **95,** 721–725.
36. Bendriem, B., Dewey, S. L., Schlyer, D. J., Wolf, A. P. & Volkow, N. D. (1991) *IEEE Trans. Nucl. Sci.* **10,** 216–222.
37. Reivich, M., Alavi, A., Wolf, A., Fowler, J., Russell, J., Arnett, C., MacGregor, R. R., Shiue, C. Y., Atkins, H., Anand, A., *et al.* (1985) *J. Cereb. Blood Flow Metab.* **5,** 179–192.
38. Rousset, O. G., Ma, Y. & Evans, A. C. (1998) *J. Nucl. Med.* **39,** 904–911.
39. Morris, J. C., Storandt, M., Miller, P., McKeel, D. W., Price, J. L., Rubin, E. H. & Berg, L. (2001) *Neurology* **58,** 397–405.
40. Jack, C. R., Peterson, R. C., Xu, Y., O'Brien, P. C., Smith, G. E. & Ivnik, R. J. (2000) *Neurology* **55,** 484–489.
41. Meguro, K., Blaizot, X., Kondoh, Y., Le Mestric, C., Baron, J. C. & Chavoix, C. (1999) *Brain* **122,** 1519–1531.
42. Kluger, A., Ferris, S. H., Golomb, J., Mittelman, M. S. & Reisberg, B. (1999) *J. Geriatr. Psychiatry Neurol.* **12,** 168–179.
43. Mark, R. J., Pang, Z., Geddes, J. W., Uchida, K. & Mattson, M. P. (1997) *J. Neurosci.* **17,** 1046–1054.
44. Reiman, E. M., Uecker, A., Gonzalez-Lima, F., Minear, D., Calloway, N. P., Berndt, J. D. & Games, D. (2000) *NeuroReport* **11,** 987–991.
45. Bobinski, M., Wegiel, J., Tarnawski, M., Reisberg, B., de Leon, M. J., Miller, D. C. & Wisniewski, H. M. (1997) *J. Neuropathol. Exp. Neurol.* **56,** 414–420.
46. Tulving, E. (1985) *Am. Psychol.* **40,** 385–398.
47. de Leon, M. J., George, A. E., Tomanelli, J., Christman, D., Kluger, A., Miller, J., Ferris, S. H., Fowler, J., Brodie, J., Klinger, A., *et al.* (1987) *Neurobiol. Aging* **8,** 319–323.